Chemotactic encounters between bacteria and phytoplankton – the stakes are high for encounters with small phytoplankton.

Riccardo Foffi[a], **Douglas Brumley**[b], **François Peaudecerf**[c], **Roman Stocker**[a], **and Jonasz Słomka**[a,1]

This manuscript was compiled on September 1, 2023

Chemotaxis, the ability to navigate along chemical gradients, enables motile bacteria to increase encounters with symbiotic partners such as phytoplankton cells. However, it remains unclear how strongly chemotactic encounters depend on the bacterial strategy employed to detect noisy and spatially confined gradients around phytoplankton of different sizes. Here, we compute analytically and numerically an upper bound on the chemotactic index, a dimensionless number that measures the increase in encounter rate with a phytoplankton cell due to chemotaxis over random motility alone. We find that chemotaxis potentially strongly favors searches for small phytoplankton, owing to the ballistic nature of the encounter for those cells, but the magnitude of the chemotactic index is very sensitive to the bacterial ability to detect spatially confined gradients. For example, in productive waters, chemotaxis can decrease the search times of bacteria for micron-sized picophytoplankton by more than ten-fold, from days to a few hours. Still, this benefit of chemotaxis is easily erased – reducing by half the phytoplankton radius or doubling the bacterial swimming speed renders gradients undetectable. For larger phytoplankton (radius $\sim 30\,\mu$m), the decrease in the search time is more moderate, from a month to a week, and depends gently on gradient detection. Thus, engaging chemotaxis in interactions with small phytoplankton is a high-stakes game for bacteria: the potential payoff is large, but it changes abruptly with bacterial ability to sense gradients, a scenario that may promote a diversity of chemotactic strategies.

encounter rates | chemotaxis | bacteria-phytoplankton interactions | microbial ecology

Significance Statement

Authors must submit a 120-word maximum statement about the significance of their research paper written at a level understandable to an undergraduate educated scientist outside their field of speciality. The primary goal of the significance statement is to explain the relevance of the work in broad context to a broad readership. The significance statement appears in the paper itself and is required for all research papers.

Chemotaxis is a widespread mechanism in motile microorganisms to detect and navigate chemical gradients (). In bacteria, chemotaxis operates by sensing temporal changes in the concentration of chemoattractant compounds (1, 2) and biasing bacterial motion towards regions where attractant concentrations are higher.

Based on a molecule counting process, chemotaxis is inherently subject to noise, especially at low attractant concentrations (3, 4). The limits that noise imposes on chemosensing are well characterized for wide, linear concentration ramps, typical of classical laboratory assays (5), and for intense but short-lived gaussian pulses, comparable to cell lysis events (6, 7). The importance of noise for chemotaxis can be especially appreciated in oceanic environments, where nutrient concentrations are often extremely low () and being able to cut through the noise and increase the probability to encounter a nutrient hotspot or a symbiotic partner can determine life or death for a bacterium (8).

In the water column, phytoplankton cells generate complex chemical landscapes by leaking dissolved organic compounds which can be strong attractants for bacteria (9–11). The ability of bacteria to navigate these gradients and reach proximity with phytoplankton cells can be crucial for establishing symbiotic relationships and favoring metabolic exchanges (12, 13) which lie at the heart of oceanic carbon cycles (14). The composition of marine phytoplankton communities can span up to two orders of magnitude in cell size, from $\sim 0.5\,\mu$m to $\sim 100\,\mu$m, with the smallest cells being by far the most abundant (15, 16). While larger cells may easily produce gradients extending from tens to hundreds of microns, the

Author affiliations: [a]Institute of Environmental Engineering, Department of Civil, Environmental and Geomatic Engineering, ETH Zürich, 8093 Zürich, Switzerland; [b]School of Mathematics and Statistics, The University of Melbourne, Parkville, Victoria, Australia; [c]Univ Rennes, CNRS, IPR (Institut de Physique de Rennes) - UMR 6251, F-35000 Rennes, France

Please provide details of author contributions here.

Please declare any competing interests here.

[1]To whom correspondence should be addressed. E-mail: jonasz.slomka@gmail.com

DRAFT

chemoattractant fields produced by the micron-sized picoplankton may be relatively weak and/or confined to small spatial regions, requiring chemotactic bacteria to tackle the additional problem of spatial resolution, a significantly different scenario from those that have been classically investigated. How sensing noise and spatial confinement jointly affect the success of bacterial chemotactic searches across the water column is therefore unclear.

Here we investigate how chemotaxis can increase encounter rates between bacteria and phytoplankton cells. Combining constraints on the detection of noisy and spatially confined gradients with the size-dependent nature of random encounters, we obtain an upper bound to the possible increase in encounter rates resulting from the use of chemotaxis, with respect to purely random searches. Our results, also supported by a numerical model of an ideal sensor, paint a picture of chemotactic encounters as an asymmetric evolutionary game. Chemotaxis towards large phytoplankton cells offers easily accessible but modest reductions in search times; search times for the ~~small~~ picoplankton can instead decrease drastically although the risk of failure is high.

Phytoplankton of different sizes generate chemical gradients of varying steepness and spatial extent, posing fundamentally different gradient detection challenges for bacteria. Using idealized models of bacterial and phytoplankton behavior, we design a system where the bacterium is performing a random exploration of the environment and employs chemotaxis to guide its motion towards the target phytoplankton cell which is leaking chemoattractant (Fig. 1). A bacterium is a spherical particle of radius $a = 0.5\,\mu\text{m}$ (assumed fixed throughout the article), which, in the absence of chemoattractant fields, performs a random walk with speed U and correlation length λ. A phytoplankton cell is a spherical particle of radius R which, exuding organic compounds through its cell wall at constant rate, generates a stationary spatial field of chemoattractant of the form

$$C(r) = C_0 + C_s \frac{R}{r} \qquad [1]$$

where C_0 is the background concentration of the compound, far away from the phytoplankton cell, C_s is the excess concentration of the compound at the phytoplankton cell surface, and r is the radial distance from the center of the phytoplankton cell. We assume that the organisms are in a quiescent environment where no mixing occurs (17). The search is terminated when an encounter, i.e. physical contact, between the bacterium and the target phytoplankton cell occurs. We ignore any possible mechanical effects due to the low-Reynolds motion of the bacterium (18) or due to the increased viscosity and mucus-like properties of the medium in the immediate surroundings of the phytoplankton cell (19**?**). To avoid the intricacies associated to the spatio-temporal and orientational dependencies of chemotactic behavior (20), we consider the bacterium to be a "perfect chemotaxer": there exists a distance S from the phytoplankton cell at which the gradient becomes strong enough to be reliably detected, and the bacterium is able to exploit it to produce an encounter with 100% probability (Fig. 1A). We call this distance S the "sensory distance". The core assumption is that no chemotactic behavior is manifested outside this sensory distance. This limit effectively simplifies the problem of gradient detection and navigation to only that of gradient detection, and we will only need to define how large this sensory distance is. As soon as the sensory distance is reached, we can consider the encounter to have happened, obtaining an upper bound to the performance of chemotactic searches. Bacteria use encounters with attractant molecules to estimate the local chemical gradient. The rate of such encounters is determined by the local concentration of the attractant compound (Eq. 1) and the diffusivity of the compound, D_c (Fig. 1A inset), independently of the swimming speed of the bacterium (3).

During navigation, the individual adsorption events of chemoattractant molecules generate a time sequence which the bacterium has to process in order to obtain an estimate of the concentration gradient () (Fig. 1B). The signal processing occurs over a characteristic sensory timescale T limited by the diffusion of CheY-P through the cytoplasm, with typical values between 50 and 100 ms (21). Even without taking into account the actual chemotactic response function (22, 23), the sensory timescale T determines how the bacterium perceives its local environment. Since larger cells contain higher amounts of carbon (24), they can release larger concentration of chemoattractants extending over wide spatial regions, while the fields produced by smaller cells are likely to be weaker and more localized in space. Therefore, a bacterium moving in the chemoattractant field generated by a large phytoplankton cell will experience a large baseline adsorption rate with only a gradual increase over time, whereas in the case of a small phytoplankton cell the signal will mostly be indistinguishable from the background, until, at very close distance from the phytoplankter, the bacterium will experience a sudden burst in adsorption events localized within a single sensory window. Phytoplankton cells at the two extrema of the size spectrum can therefore produce gradients whose features pose different fundamental limits on bacterial chemotactic performance. Gradients generated by large cells lead to the classical "gradient climbing" problem, and their detection is only limited by the relationship between the inherent sensing noise and the gradient steepness (5). We propose that gradients generated by small cells are instead limited by "resolution": during a single sensory window T the bacterium travels a distance $\Delta x = UT$; when this distance is comparable or larger than the spatial extent of the gradient, then the bacterium might not be able to robustly detect the gradient, in the same way that sampling a signal below its Nyquist frequency will produce a distorted representation of the signal itself ().

Chemotactic performance is limited by random encounters with the sensory distance at which bacteria detect chemical gradients. The intuition about these two distinct limits of gradient detection can be translated into a performance landscape, where the ability of bacteria to detect a gradient is represented as a function of the phytoplankton radius R and the strength of the chemoattractant field it produces, parameterized by the excess concentration C_s (Fig. 2). The detectability of a gradient is determined by the condition that its signal-to-noise ratio (SNR) be larger than some fixed value q, and that its spatial extent (represented by the sensory distance S) be larger than the distance traveled by the bacterium during the sensory timescale T (see SI for detailed discussion). For any given radius R, there will be a minimum concentration C_s for the gradient to be detectable. For large phytoplankton cells, increasing C_s increases the steepness of the gradient; for small phytoplankton cells the gradients are already steep and increasing C_s leads to spatial expansion. Independently of the

DRAFT

details of the signal processing mechanism, these two limits will define a convex region (delimited by the thick black boundary in Fig. 2) where gradients can be detected. Within this region of detectability, the performance of a chemotactic search is quantified by the chemotactic index I_c, that is the ratio between the rate of chemotactic and random encounters. The rate of random encounters with a phytoplankton cell of radius R is independent of C_s (since chemotaxis is not employed by the bacterium); these rates can be quantified by encounter kernels (i.e. the rate of encounters per unit concentration of target and searcher), which take a different form depending on the relationship between phytoplankton radius R and the correlation length of the bacterial random walk λ (25). When the phytoplankton is small compared to the bacterial correlation length ($R < \lambda$) the encounters are ballistic and are described by the kernel $\pi U R^2$ (26); for larger phytoplankton cells ($R > \lambda$) the encounters are of diffusive nature and described by the kernel $4\pi D R$ (27) where $D = U\lambda/3$ is the effective diffusivity of the bacterium (28). Since bacterial behavior outside the sensory distance S is assumed to be completely random, chemotactic encounters with the target phytoplankton are equivalent to random encounters with the sensory sphere of radius S and are therefore also described by random encounter kernels, allowing us to obtain upper bounds to the value of the chemotactic index I_c. If a small phytoplankton cell generates a chemoattractant field which is wide enough to be detected, but whose spatial extension is still smaller than the bacterial correlation length ($R < S < \lambda$, subregion 1 in Fig. 2) then both random and chemotactic encounters are ballistic, giving

$$I_c = \frac{S^2}{R^2}. \qquad [2]$$

For a large phytoplankton cell ($R > \lambda$) the sensory distance can only be further larger ($S > R > \lambda$, subregion 2 in Fig. 2) so that both random and chemotactic encounters are diffusive, leading only to a linear scaling

$$I_c = \frac{S}{R}. \qquad [3]$$

A third scenario (not shown in Fig. 2) is for small cells whose chemoattractant field is strong enough to be associated with a sensory distance $S > \lambda > R$, in which case random encounters are ballistic while chemotactic encounters are diffusive, resulting in a chemotactic index

$$I_c = \frac{4}{3}\frac{\lambda S}{R^2}. \qquad [4]$$

As we will see later, this situation is rare in realistic scenarios for bacteria-phytoplankton encounters and therefore we will only focus on the purely-ballistic and purely-diffusive types of encounters of Eq. 2 and 3. Estimates of the chemotactic index I_c are therefore subordinate to a definition of the sensory distance S.

The sensory distance S is a simultaneous measure of both how strong the chemoattractant field from the phytoplankton is, and how well the bacterium is able to measure it. For a bacterium swimming with speed U in the stationary chemoattractant field $C(r)$, the instantaneous estimate of the temporal gradient is obtained as the convective derivative of the field $\mathrm{d}C/\mathrm{d}t = U\nabla C$; the lower limit to the inherent noise in the gradient measurement was computed by Mora & Wingreen (5) as $\sigma_0 = \sqrt{3C/(\pi a D_c T^3)}$, and Brumley et al. (7) have later shown that in marine bacteria the sensing noise could be well approximated by multiplying this σ_0 by a "chemotactic precision" factor giving $\sigma = \Pi\sigma_0$ with typical values $\Pi \approx 6$. We use the signal-to-noise ratio $\mathrm{SNR} = U\nabla C/\Pi\sigma_0$, multiplied by a cutoff function $f_c(x) = 1 - \exp\left(-x^{3/2}\right)$ to define the sensory distance. S is therefore the solution to the equation

$$\frac{U\nabla C(S)}{\Pi\sigma_0(S)} f_c(S/UT) = q \qquad [5]$$

for some value of the threshold q. Throughout this article, we fix $q = 1$ and $\Pi = 6$. See SI for more details. Once the values of S have been evaluated (Fig. SX), they can be used to compute the chemotactic index.

The performance landscape for chemotactic bacteria-phytoplankton encounters has a convex landscape and displays clear qualitative differences between the small-radii and the large-radii region (Fig. 3A). Contour lines of the I_c profile have a higher density close to the detection boundary in the region of small phytoplankton radii, suggesting that modest variations in the excess concentration C_s leaked by a small phytoplankter can have huge impacts on the performance of bacterial chemotaxis. Indeed, ~~the~~ I_c has a much sharper dependency on C_s when the phytoplankton radius R is small, and especially so when crossing the detection boundary (Fig. 3B): while a bacterium might not be able to sense ($I_c = 1$) an attractant gradient from a 1 µm phytoplankter leaking with $C_s = 10\,\mathrm{nM}$, a few nM increase can quickly enhance the I_c to values of 10 and more; as C_s is further increased we get deeper into sensing territory, and the dependecy of I_c on C_s quickly smooths out. For larger phytoplankton cells, there is no sharp increase: when the boundary of detection is crossed, the I_c only grows gradually with C_s. Simultaneously, for small values of the excess concentration C_s, an increase in phytoplankton radius R leads first to a sharp increase in chemotactic index and then a gradual decrease towards $I_c = 1$ when R overcomes an optimal value (Fig. 3C). As C_s is increased, phytoplankton cells with smaller sizes keep offering disproportionately larger advantages to chemotactic performance compared to the larger cells whose detection requires larger and larger values of C_s. These results suggest that investing in chemotaxis towards small phytoplankton cells could be a risky business for bacteria, but with potentially much higher gains (in terms of number of encounters) compared to the safe but low-rewarding larger cells. The same also applies in reverse: if a small phytoplankton cell wants to attract bacteria, slightly tuning up their leakage can drastically increase the number of incoming bacteria; a larger phytoplankton cell would need to leak disproportionately more for a comparable increase in encounters. Such an asymmetric performance landscape might have supported the evolution of a diversity of chemotactic strategies.

Variations in search strategies, defined by parameters such as swimming speed U, sensory timescale T or compound diffusivity T, determine the benefits of chemotaxis for a given phytoplankton radius and excess concentration, but don't affect the fundamental structure of the performance landscape (Fig. 4). A reduction in sensory timescale from 100 to 50 ms significantly decreases bacterial ability to detect gradients from large phytoplankton cells and reduces the overall performance of chemotaxis (Fig. 4A). An increase in swimming speed from 50 to 100 $\mu\mathrm{m\,s}^{-1}$ improves the performance of chemotaxis within the region of detectability, but the region itself is shifted

DRAFT

towards larger radii values, highlighting a tradeoff between degraded spatial resolution and improved sensing accuracy (Fig. 4B). An increase in the diffusivity of the chemoattractant compound from 500 to 1000 $\mu m^2/s$ enhances the signal-to-noise ratio without affecting spatial resolution, and it thus shifts the region of detectability towards lower C_s values (Fig. 4C). Unaffected by the variation in these quantities, the high-stakes nature of chemotactic searches towards small phytoplankton cells is therefore only a direct result of the sharp cutoff on spatial resolution combined with the quadratic scaling of the I_c associated to ballistic encounters.

The generality of these results is supported by a numerical model of an ideal sensor which has no direct relationship to bacterial chemosensory mechanisms (Fig. 4D–F). This ideal sensor is defined as a sphere moving at constant speed U towards a phytoplankton cell leaking a chemoattractant field $C(r)$. As it moves, the sensor registers all the adsorption events of chemoattractant molecules, occurring with instantaneous rate $4\pi D_c a C(r)$. After an interval of length T, the registered events are processed and a new acquisition starts. For the signal processing, the sensor performs a one-sided Kolmogorov-Smirnov test (29) comparing the distribution of the waiting times between the freshly-collected events, with the distribution recorded in the previous acquisition window. If the cumulative distribution function in the new interval is found to be larger than that in the previous interval, then the sensor has detected a gradient. Averaging the successful gradient detections over an ensemble of such ideal sensors provides an estimate of the sensory distance S, defined as the largest distance where at least a fraction f of the sensors has detected a gradient. The estimates of S can then be used to estimate the chemotactic index I_c. Remarkably, we find that choosing a high consensus threshold $f = 0.99$ provides close agreement with our theoretical calculations, both in terms of the shape of the detectability region and of the estimated I_c values. This fact highlights how the detection limits evaluated for bacterial chemosensing and the asymmetric nature of the chemotactic performance are not actually specific to bacteria, but can be used to describe a wide class of systems estimating gradients through temporal comparisons, independently of the particular signal processing mechanism and navigation parameters.

Section 'Search timescales in realistic conditions'.

While our theoretical investigation has provided general insight about the behavior of encounters assisted by chemosensory mechanisms over a broad range of radii R and excess concentration values C_s, phytoplankton cells will only be found in a limited region of values. Using empirical carbon-size scaling laws (24, 30), each phytoplankton cell size R can be associated to a given carbon content. At any time, a fixed fraction of the total carbon content of the cell, termed the percent extracellular release (PER), is assumed to be exuded with a constant rate, which then defines the value of the excess concentration at surface C_s. Average values of the percent extracellular release are expected to be around 20%, but variations between values of PER $\approx$ 2% and 50% are typical and also strongly dependent on physiological and environmental conditions (31). This physiological range of exudation rates for healthy phytoplankton cells lies across the boundary of chemotactic detection (Fig. 5A), suggesting that chemotaxis might play a relevant role for encounters across the entire size spectrum.

In addition to the increase in encounters provided by chemotaxis as measured by the chemotactic index I_c, we want to estimate the actual rate at which such encounters occur in the ocean, or equivalently, the average time a bacterium needs to search before encountering a phytoplankton cell. The average search time required by a bacterium to encounter a phytoplankton cell can be obtained as

$$T_e = \frac{1}{I_c \Gamma N} \qquad [6]$$

where Γ is the random encounter kernel between the bacterium and the phytoplankton and N is the phytoplankton concentration. Marine phytoplankton communities have characteristic size structures which usually follow a power-law size-abundance relationship of the form $N(R) \propto R^{-3\alpha}$, where the allometric exponent α takes typical values $\alpha \approx 0.9$ in oligotrophic waters and $\alpha \approx 0.75$ in productive waters (16). Phytoplankton cells with smaller radii are therefore vastly more abundant than cells with larger radii, and particularly so in oligotrophic environments where large phytoplankters are extremely rare (Fig. 5B).

The steep size-structure of phytoplankton communities clearly favors encounters with the smaller phytoplankton even in the absence of chemotaxis (Fig. 5C–D, thin lines). In oligotrophic waters, a bacterium swimming randomly with speed 40 $\mu m\, s^{-1}$ can encounter a 0.5 µm phytoplankton roughly every 100 hours, while encountering a 30 µm phytoplankton will take on average more than a month. In productive waters the search times for small cells are only slightly higher, whereas those for larger cells fall down below a month. Bacteria with a higher swimming speed of 80 $\mu m\, s^{-1}$ reduce their random search times due to improved exploration efficiency although that comes with a tradeoff in terms of chemotactic performance, as also shown in Fig. 4B. The decreases in search times resulting from the use of chemotaxis, over the whole range of phytoplankton PER values, are shown as shaded bands in Fig. 5C and D. Bacteria with smaller speed but longer sensory timescales T can decrease their search times for the smallest phytoplankton by a factor 10, whereas the faster swimming bacteria with a shorter sensory timescale cannot benefit at all from chemotaxis at this extreme of the spectrum. The importance of this apparently tiny difference (as seen by the difference in the green and violet bands of Fig. 5C and D), is better understood by realizing that the smallest cells constitute the vast majority of the population. The 95th percentile of the populations (marked by the dotted vertical lines in the figures) is below the 2 µm radius, and, in both environments, more than half of the population is contained within the first size class. Therefore, losing the ability to increase encounters with the smallest cells in the spectrum can dramatically impact the dynamics of the population. These rather general features of chemotaxis-assisted encounters may support and even promote the coexistence between generalist bacteria, with phenotypes better suited to increase encounters over the entire size spectrum, and specialist bacteria which optimize their performance in the low-end of the spectrum, where the competition is strongest.

Using idealized models of phytoplankton leakage and bacterial chemotaxis, we have identified fundamental limits to the ability of bacteria to detect gradients and used them

DRAFT

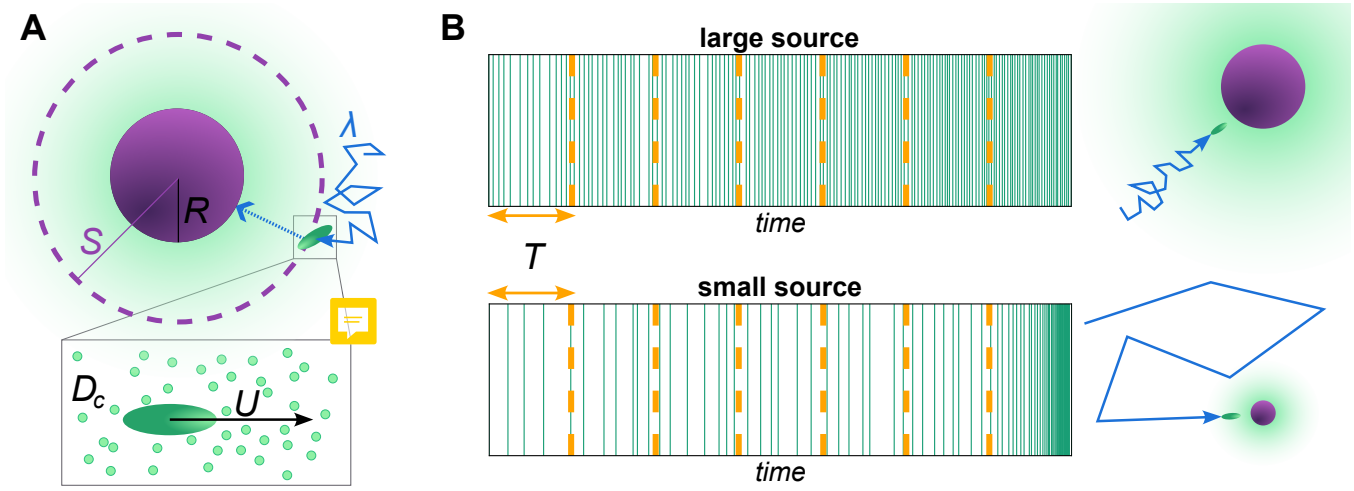

Fig. 1. Detecting chemical gradients to increase encounter rates with phytoplankton is a size-dependent challenge for bacteria. (A) A phytoplankton cell of radius R produces a stationary diffusive field of a chemoattractant, $C(r) = C_0 + C_s R/r$ (represented by the green halo). Far away from the cell, bacteria cannot sense the chemoattractant and thus swim in random walks, with correlation length λ. The "sensory distance" S is the distance from the phytoplankton cell at which a perfect chemotaxer would be able to detect the gradient and encounter its target with a 100% probability. (Inset) Chemosensing is a molecule-counting process based on encounters between the bacterium and individual chemoattractant molecules. Attractant molecules reach the bacterium via diffusion (diffusivity D_c) while the bacterium swims at speed U through the chemoattractant field. (B) Encounters with individual attractant molecules result in a sequence of absorption events (each event represented by a spike in the plots). The bacterial chemosensory machinery integrates these sequences over a characteristic sensory timescale T to produce an estimate of the local concentration gradient. The phytoplankton size determines the lengthscale over which the gradients establish, leading to absorption sequences with well-distinguished features for small and large sources.

to establish upper bounds to the enhancement in bacteria-phytoplankton encounters driven by chemotaxis. Comparing our bacteria-specific theoretical calculations to a biology-agnostic model of an ideal sensor, we have shown that the features of the chemotactic performance landscape, namely the sharp sensitivity of chemotactic performance towards small phytoplankton cells opposed to the smooth but modest performance increases obtained for the large phytoplankton, may be common to a broad class of sensory systems based on temporal gradient sensing. In particular, the sharp cutoff in sensing ability due to gradient confinement and the quadratic scaling of the chemotactic index resulting from the ballistic nature of encounters, drive a strong competition in the search for small targets.

It is suggestive to think of the chemotactic encounter problem as an evolutionary game with a strongly asymmetric fitness function. When searching for small cells there is no middle ground, the fitness of a given search strategy quickly jumps from null ($I_c = 1$) to extremely high.

Results

Discussion

Author Affiliations. Include department, institution, and complete address, with the ZIP/postal code, for each author. Use lower case letters to match authors with institutions, as shown in the example. PNAS strongly encourages authors to supply an ORCID identifier for each author. Individual authors must link their ORCID account to their PNAS account at www.pnascentral.org. For proper authentication, authors must provide their ORCID at submission and are not permitted to add ORCIDs on proofs.

Digital Figures. EPS, high-resolution PDF, and PowerPoint are preferred formats for figures that will be used in the main

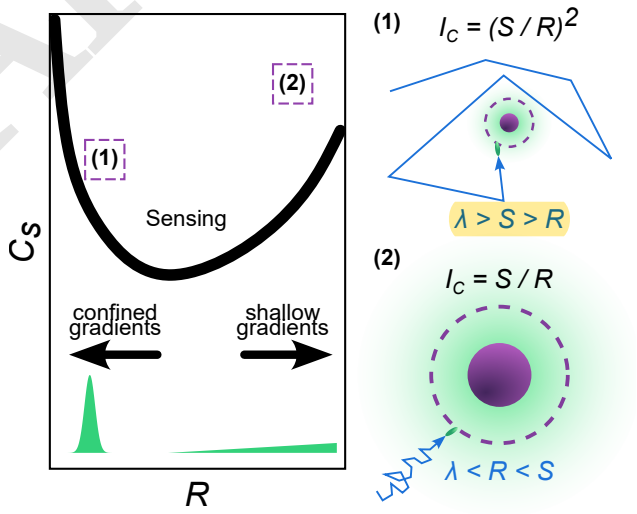

Fig. 2. Chemotactic encounters are limited by the gradients' steepness and spatial extent, and ballistic or diffusive encounters with the phycosphere. Schematic depiction of the performance landscape for chemotactic searches. The source size R and the chemoattractant concentration C_s determine whether gradients can be successfully detected or not. The thick black line defines the boundary of detection, separating the regions where gradient detection is or is not possible. Below the boundary, two conditions limit an organism's ability to perform chemotaxis: gradients are either too spatially confined or too shallow. In this region, chemotaxis provides no benefit over random motility. Above the boundary, gradients can be detected, and the increase in encounters compared to random motility, measured by the chemotactic index I_c, is determined by the relationship between bacterial correlation length λ, source size R and sensory radius S. Small sources (subregion 1) lead to ballistic encounters for which the chemotactic index scales quadratically with the sensory radius S, whereas for large sources (subregion 2) the chemotactic index scales only linearly with S due to the diffusive nature of encounters.

DRAFT

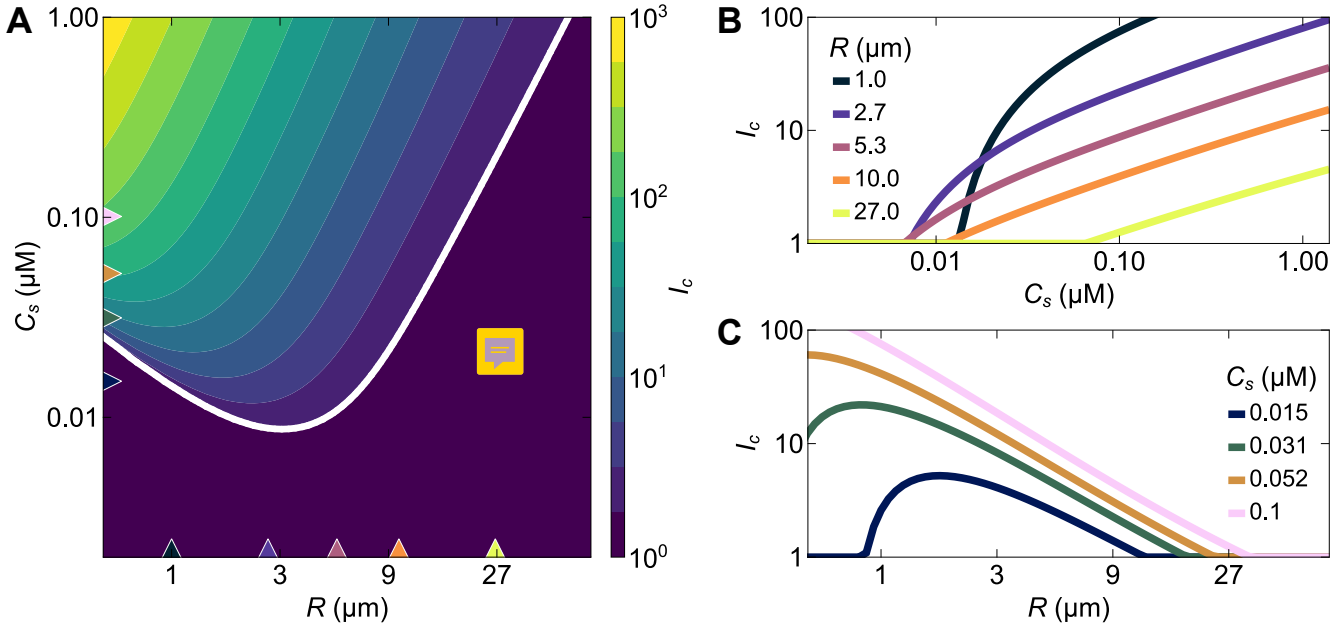

Fig. 3. The stakes are high for encounters with small phytoplankton – the slope of the chemotactic index is steep for small but gentle for large phytoplankton. (A) Performance (I_c) landscape for a bacterium using chemotaxis to drive encounters with spherical targets of different radii (R) and chemoattractant concentrations (C_s). The thick white line defines the boundary of detection, separating the region where gradients are detectable and chemotaxis is beneficial to encounters ($I_c > 1$) from the region where gradients are too shallow or too spatially confined to be detected ($I_c = 1$). (B) Vertical transects from panel A for fixed values of the target radius R (corresponding to the upward-pointing triangles). In chemotaxis towards small targets, a slight variation in the chemoattractant concentration can make the difference between a highly successful search ($I_c \sim 10$) or a failure ($I_c = 1$), whereas for larger targets the dependency of I_c on the chemoattractant concentration is more gradual. (C) Horizontal transects from panel A for fixed values of the chemoattractant concentration C_s (corresponding to the right-pointing triangles). For weak sources, an increase in size R produces initially large enhancements in chemotactic performance, with diminishing returns upon further enlargement. As the source gets stronger, the increase in performance for chemotaxis towards small targets becomes disproportionately larger; larger sources also become detectable although offering modest performance improvements over random searches.

manuscript. Authors may submit PRC or U3D files for 3D images; these must be accompanied by 2D representations in TIFF, EPS, or high-resolution PDF format. Color images must be in RGB (red, green, blue) mode. Include the font files for any text.

Images must be provided at final size, preferably 1 column width (8.7cm). Figures wider than 1 column should be sized to 11.4cm or 17.8cm wide. Numbers, letters, and symbols should be no smaller than 6 points (2mm) and no larger than 12 points (6mm) after reduction and must be consistent.

Supporting Information Appendix (SI). Authors should submit SI as a single separate SI Appendix PDF file, combining all text, figures, tables, movie legends, and SI references. SI will be published as provided by the authors; it will not be edited or composed. Additional details can be found in the PNAS Author Center. The PNAS Overleaf SI template can be found here. Refer to the SI Appendix in the manuscript at an appropriate point in the text. Number supporting figures and tables starting with S1, S2, etc.

Authors who place detailed materials and methods in an SI Appendix must provide sufficient detail in the main text methods to enable a reader to follow the logic of the procedures and results and also must reference the SI methods. If a paper is fundamentally a study of a new method or technique, then the methods must be described completely in the main text.

Materials and Methods

Please describe your materials and methods here. This can be more than one paragraph, and may contain subsections and equations as required.

Subsection for Method. Example text for subsection.

ACKNOWLEDGMENTS. R.F. acknowledges funding from the European Union's Horizon 2020 research and innovation programme under Marie Skłodowska-Curie grant no. 955910. R.S. acknowledges... J.S. acknowledges... We also gratefully acknowledge ETH Zürich (Euler cluster) for providing computational resources.

1. RM Macnab, DE Koshland, The Gradient-Sensing Mechanism in Bacterial Chemotaxis. *Proc. Natl. Acad. Sci. USA* **69**, 2509–2512 (1972).
2. DA Brown, HC Berg, Temporal Stimulation of Chemotaxis in *Escherichia coli*. *Proc. Natl. Acad. Sci. USA* **71**, 1388–1392 (1974).
3. H Berg, E Purcell, Physics of chemoreception. *Biophys. J.* **20**, 193–219 (1977).
4. PR ten Wolde, NB Becker, TE Ouldridge, A Mugler, Fundamental Limits to Cellular Sensing. *J. Stat. Phys.* **162**, 1395–1424 (2016).
5. T Mora, NS Wingreen, Limits of Sensing Temporal Concentration Changes by Single Cells. *Phys. Rev. Lett.* **104**, 248101 (2010).
6. AM Hein, DR Brumley, F Carrara, R Stocker, SA Levin, Physical limits on bacterial navigation in dynamic environments. *J. R. Soc. Interface* **13**, 20150844 (2016).
7. DR Brumley, et al., Bacteria push the limits of chemotactic precision to navigate dynamic chemical gradients. *Proc. Natl. Acad. Sci. USA* **116**, 10792–10797 (2019).
8. DR Brumley, et al., Cutting Through the Noise: Bacterial Chemotaxis in Marine Microenvironments. *Front. Mar. Sci.* **7**, 527 (2020).
9. DC Thornton, Dissolved organic matter (DOM) release by phytoplankton in the contemporary and future ocean. *Eur. J. Phycol.* **49**, 20–46 (2014).
10. S Smriga, VI Fernandez, JG Mitchell, R Stocker, Chemotaxis toward phytoplankton drives organic matter partitioning among marine bacteria. *Proc. Natl. Acad. Sci. USA* **113**, 1576–1581 (2016).
11. JR Seymour, SA Amin, JB Raina, R Stocker, Zooming in on the phycosphere: The ecological interface for phytoplankton–bacteria relationships. *Nat. Microbiol.* **2**, 17065 (2017).
12. JB Raina, V Fernandez, B Lambert, R Stocker, JR Seymour, The role of microbial motility and chemotaxis in symbiosis. *Nat. Rev. Microbiol.* **17**, 284–294 (2019).
13. JB Raina, et al., Chemotaxis shapes the microscale organization of the ocean's microbiome. *Nature* (2022).

DRAFT

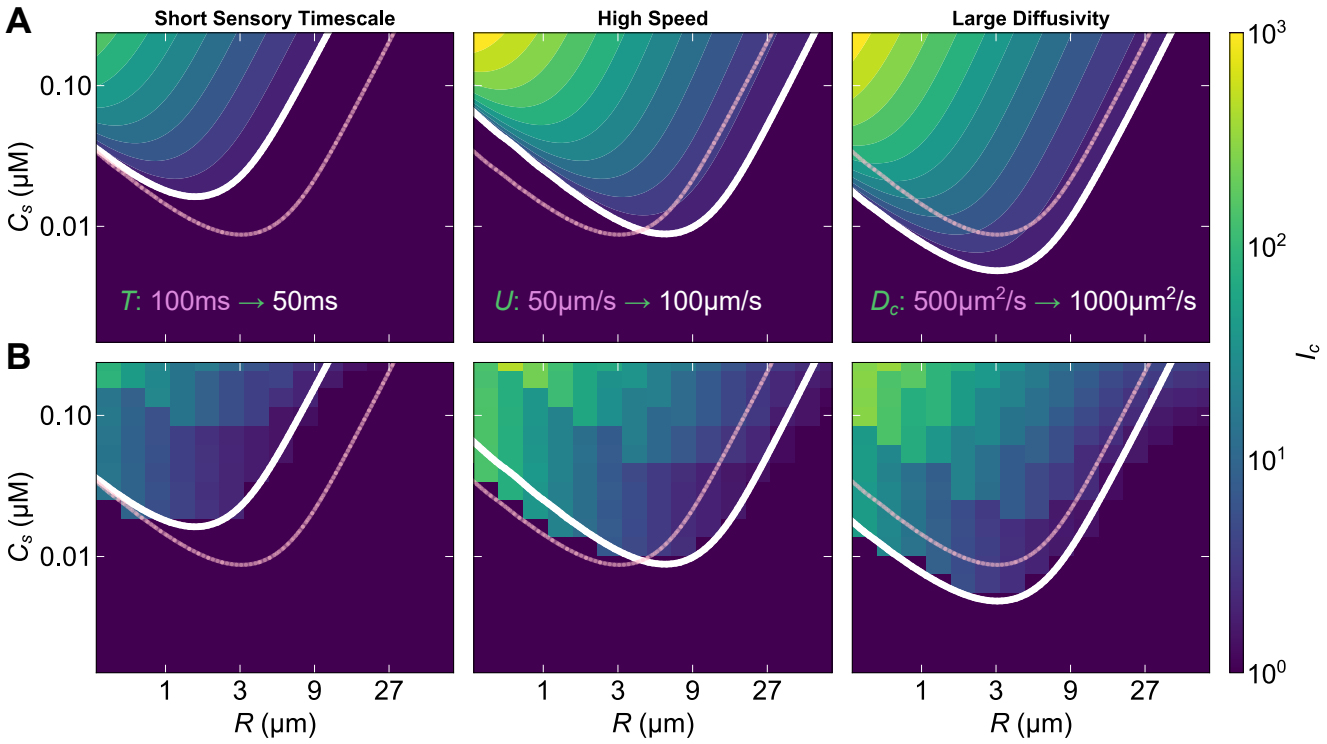

Fig. 4. Bacterial chemotactic strategy controls the chemotactic index but does not alter the high-stakes nature of encounters with small phytoplankton. Performance landscapes of different chemotactic strategies obtained from (A–C) theoretical and (D–F) computational models. In all the panels, the pink curve is the detection boundary for a reference strategy with parameter values $U = 50\,\mu\mathrm{m\,s^{-1}}$, $T = 100\,\mathrm{ms}$, $D_c = 500\,\mu\mathrm{m^2/s}$. (A) Reduction in sensory timescale T from $100\,\mathrm{ms}$ to $50\,\mathrm{ms}$. (B) Increase in swimming speed from $50\,\mu\mathrm{m\,s^{-1}}$ to $100\,\mu\mathrm{m\,s^{-1}}$. (C) Increase in chemoattractant diffusivity from $500\,\mu\mathrm{m^2/s}$ to $1000\,\mu\mathrm{m^2/s}$. (D–F) Theoretically predicted features of bacterial chemotactic performance are reproduced by an ideal sensor based on the Kolmogorov-Smirnov test. In panels D to F, the white line is the detection boundary from the theoretical prediction of panels A to C, respectively. Despite small quantitative differences in the estimated I_c values, arising from the distinct signal processing mechanism and the finite spatial resolution of numerical simulations, the features of the performance landscape are clearly conserved.

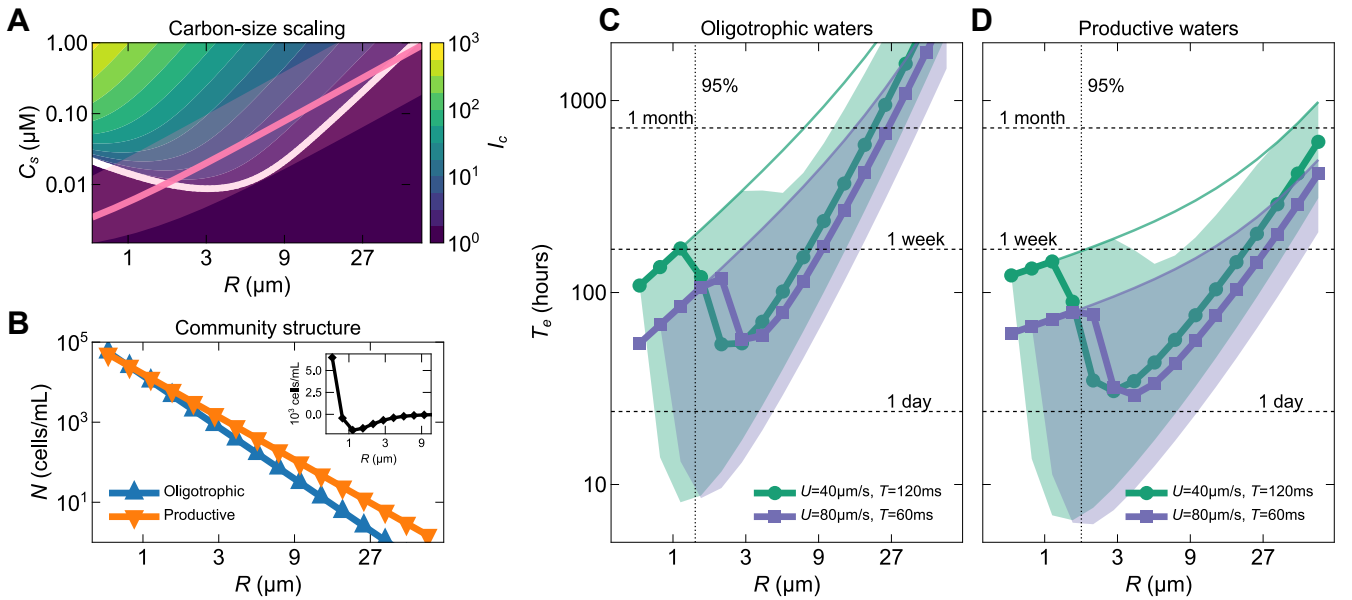

Fig. 5. The high-stakes nature of phytoplankton-bacteria interactions may promote a diversity of chemotactic strategies. (A) Characteristic values of size and released chemoattractant for phytoplankton cells resulting from carbon-size scaling laws overlaid on the performance landscape of a bacterium with swimming speed $U = 50\,\mu\mathrm{m\,s}^{-1}$, sensory timescale $T = 100\,\mathrm{ms}$, and chemoattractant diffusivity $D_c = 500\,\mu\mathrm{m}^2/\mathrm{s}$. The thick pink line corresponds to phytoplankton cells with a percent extracellular release of 10%, the shaded pink band represents variations in the percent extracellular release between 2% (lower limit) and 50% (upper limit). (B) Marine phytoplankton communities display power-law size-structures where the abundance N decreases with increasing size R as $N(R) \propto R^{-3\alpha}$. The allometric exponent is larger in oligotrophic waters ($\alpha \simeq 0.9$) than in more productive waters ($\alpha \simeq 0.75$). Both communities are normalized to a total cell abundance of $1 \times 10^5\,\mathrm{cells/mL}$. (C-D) Carbon-size scaling, phytoplankton community structure and chemotactic index jointly define the average search time (T_e) for an individual bacterium to encounter a phytoplankton cell using chemotaxis. The search time for a given phytoplankton size class is evaluated as $T_e = 1/(I_c \Gamma N)$ where Γ is the random encounter kernel and N is the abundance of phytoplankton cells in that size class. The thin solid lines represent the search times in the absence of chemotaxis ($I_c = 1$). The thick lines with markers indicate phytoplankton cells with percent extracellular release of 10% (corresponding to the thick pink line in panel A), and the shaded bands represent variations in percent extracellular release between 2% and 5% (matching the pink shaded band in panel A). The two curves corresponds to distinct chemotactic strategies: in green with circle markers a strategy with low speed and long sensory timescale; in violet with square markers a strategy with high swimming speed and short sensory timescale. The vertical dotted lines mark the radius corresponding to the 95$^{\mathrm{th}}$ percentile of the phytoplankton community abundance.

14. F Azam, Microbial Control of Oceanic Carbon Flux: The Plot Thickens. *Science* **280**, 694–696 (1998).
15. WG Sprules, M Munawar, Plankton Size Spectra in Relation to Ecosystem Productivity, Size, and Perturbation. *Can. J. Fish. Aquat. Sci.* **43**, 1789–1794 (1986).
16. P Cermeño, F Figueiras, Species richness and cell-size distribution: Size structure of phytoplankton communities. *Mar. Ecol. Prog. Ser.* **357**, 79–85 (2008).
17. JR Taylor, R Stocker, Trade-Offs of Chemotactic Foraging in Turbulent Water. *Science* **338**, 675–679 (2012).
18. EM Purcell, Life at low reynolds number. *Am. J. Phys.* **45**, 3–11 (1977).
19. F Azam, F Malfatti, Microbial structuring of marine ecosystems. *Nat. Rev. Microbiol.* **5**, 782–791 (2007).
20. MJ Schnitzer, Theory of continuum random walks and application to chemotaxis. *Phys. Rev. E* **48**, 2553–2568 (1993).
21. V Sourjik, HC Berg, Binding of the *Escherichia coli* response regulator CheY to its target measured *in vivo* by fluorescence resonance energy transfer. *Proc. Natl. Acad. Sci. USA* **99**, 12669–12674 (2002).
22. JE Segall, SM Block, HC Berg, Temporal comparisons in bacterial chemotaxis. *Proc. Natl. Acad. Sci. USA* **83**, 8987–8991 (1986).
23. PG de Gennes, Chemotaxis: The role of internal delays. *Eur. Biophys. J.* **33**, 691–693 (2004).
24. S Menden-Deuer, EJ Lessard, Carbon to volume relationships for dinoflagellates, diatoms, and other protist plankton. *Limnol. Ocean.* **45**, 569–579 (2000).
25. J Słomka, et al., Encounter rates prime interactions between microorganisms. *Interface Focus.* **13**, 20220059 (2023).
26. JC Maxwell, V. *Illustrations of the dynamical theory of gases.* —Part I. *On the motions and collisions of perfectly elastic spheres. Lond. Edinb. Dublin philos. mag. j. sci.* **19**, 19–32 (1860).
27. S Chandrasekhar, Stochastic Problems in Physics and Astronomy. *Rev. Mod. Phys.* **15**, 1–89 (1943).
28. PS Lovely, F Dahlquist, Statistical measures of bacterial motility and chemotaxis. *J. Theor. Biol.* **50**, 477–496 (1975).
29. FJ Massey, The Kolmogorov-Smirnov Test for Goodness of Fit. *J. Am. Stat. Assoc.* **46**, 68–78 (1951).
30. MM Mullin, PR Sloan, RW Eppley, Relationship between Carbon Content, Cell Volume, and Area in Phytoplankton. *Limnol. Ocean.* **11**, 307–311 (1966).
31. E Marañón, P Cermeño, E Fernández, J Rodríguez, L Zabala, Significance and mechanisms of photosynthetic production of dissolved organic carbon in a coastal eutrophic ecosystem. *Limnol. Ocean.* **49**, 1652–1666 (2004).

DRAFT